Published in final edited form as:
Brain Pathol. 2008 April ; 18(2): 153–163. doi:10.1111/j.1750-3639.2007.00107.x.

Myelin Abnormalities without Oligodendrocyte Loss in Periventricular Leukomalacia

Saraid S. Billiards[1], **Robin L. Haynes**[1,2], **Rebecca D. Folkerth**[1,3], **Natalia S. Borenstein**[1], **Felicia L. Trachtenberg**[4], **David H. Rowitch**[5,6,*], **Keith L. Ligon**[1,6], **Joseph J. Volpe**[2], and **Hannah C. Kinney**[1]

[1]Department of Pathology, Children's Hospital Boston and Harvard Medical School, Boston, Mass

[2]Department of Neurology, Children's Hospital Boston and Harvard Medical School, Boston, Mass

[3]Department of Pathology, Brigham and Women's Hospital, Boston, Mass

[4]New England Research Institutes, Watertown, Mass

[5]Department of Divisions of Neonatology and Hematology, Children's Hospital Boston and Harvard Medical School, Boston, Mass

[6]Department of Pediatric Oncology, Dana-Farber Cancer Institute, Harvard Medical School, Boston, Mass

Abstract

The cellular basis of myelin deficits detected by neuroimaging in long-term survivors of periventricular leukomalacia (PVL) is poorly understood. We tested the hypothesis that oligodendrocyte lineage (OL) cell density is reduced in PVL, thereby contributing to subsequent myelin deficits. Using computer-based methods, we determined OL cell density in sections from 18 PVL and 18 age-adjusted control cases, immunostained with the OL-lineage marker Olig2. Myelination was assessed with myelin basic protein (MBP) immunostaining. We found no significant difference between PVL and control cases in Olig2 cell density in the periventricular or intragyral white matter. We did find, however, a significant increase in Olig2 cell density at the necrotic foci, compared with distant areas. Although no significant difference was found in the degree of MBP immunostaining, we observed qualitative abnormalities of MBP immunostaining in both the diffuse and necrotic components of PVL. Abnormal MBP immunostaining in PVL despite preserved Olig2 cell density may be secondary to arrested OL maturation, damage to OL processes, and/or impaired axonal-OL signaling. OL migration toward the "core" of injury may occur to replenish OL cell number. This study provides new insight into the cellular basis of the myelin deficits observed in survivors of PVL.

Keywords

Periventricular leukomalacia; oligodendrocytes; Olig2; myelin

Corresponding author: Hannah C. Kinney, MD, Department of Pathology, Enders Building, Room 1112, Children's Hospital Boston, 300 Longwood Avenue, Boston, MA 02115 (E-mail: hannah.kinney@childrens.harvard.edu).
*Present address: David H. Rowitch, MD, PhD, Department of Pediatrics, Institute for Regeneration Medicine, San Francisco, Calif.

INTRODUCTION

Periventricular leukomalacia (PVL) is the principal form of brain injury in the premature infant and the predominant pathologic finding underlying cerebral palsy. The pathogenesis of PVL likely involves multiple factors in the critically ill premature infant, including cerebral ischemia/reperfusion caused by impaired cerebrovascular autoregulation (24,49) and inflammation triggered by maternofetal infection (12,16,17,24,50). During the period when infants are at greatest risk for PVL, that is, 24–32 post-conceptional (PC) weeks, premyelinating late oligodendrocyte progenitors ($O4^+$ and $O1^+$) (preOLs) predominate in the human cerebral white matter (3). We have shown previously that these preOLs undergo oxidative and nitrative stress in PVL (19), suggesting that they are vulnerable to free radical injury.

Lethal injury to preOLs in the immature (non-myelinated) cerebral white matter has been postulated to be a key feature of PVL (18,41,49), resulting in hypomyelination, as documented by neuroimaging studies (11,13,14,21,32). Two neuropathologic studies suggest a loss of preOLs in PVL (6,19); however, the overall number of PVL cases studied in these two reports is limited. Although an earlier study by Iida et al (20) reported a loss of oligodendrocyte lineages (OLs) in a larger PVL dataset, this was determined using a non-specific OL marker, ferritin. The analysis of preOLs in human PVL has been hampered by the lack of immunological markers that can be applied to formalin-fixed and paraffin-embedded tissue (6,19). Olig2 is a basic helix-loop-helix transcription factor, essential for OL development (42). Expression of Olig2 in the vertebrate brain appears to be the earliest indicator of OL differentiation, and it continues to be expressed in many OLs of the adult brain (2,29). Thus, Olig2 serves as a marker of the OLs throughout their lineage, including mature [myelin basic protein (MBP) positive] myelinating OLs, notably in archival tissue (27,28).

In the following study, we tested the hypothesis that the density of Olig2 cells is reduced in PVL and that this reduction occurs in association with increased cell death. We further hypothesized that the severity of OL loss is dependent on the distance from the necrotic periventricular focus, that is, the closer to the focal core, the greater the reduction in OL cell density, given that the necrotic focus represents the most severe degree of tissue damage. In addition, we hypothesized that there is a reduction in the degree of MBP immunostaining in PVL cases compared with controls, which reflects in turn the putative reduction in Olig2 cell density. We recognize that the use of the Olig2 marker does not establish the specific stage of OL injury, that is, if the putative OL cell loss specifically affects O4, O1 and/or MBP-positive OLs. Therefore, we also assessed the density of O4-positive OLs in an initial study, with the hypothesis that there is a reduction in O4-positive OLs in PVL.

MATERIALS AND METHODS

Clinical database

A total of 36 cases were collected from the autopsy services of the Departments of Pathology at the Children's Hospital Boston and Brigham and Women's Hospital, Boston, MA, according to the guidelines of the Human Protection Committees at each institution. All cases were processed for standard histological examination (eg, hematoxylin and eosin/Luxol fast blue staining) to assess the classification of cases as PVL or control. Gestational ages of the fetuses were determined by clinical assessment prior to death. Age was expressed as PC weeks (gestational plus post-natal age).

Determination of histopathology

We define PVL based upon a combination of "focal" and "diffuse" components (24). The focal component is comprised of periventricular necrosis in which cellular constituents are destroyed. The diffuse component is comprised of reactive gliosis and microglial activation in the deep white matter surrounding the necrotic foci. Acute PVL is identified by coagulative necrosis with nuclear pyknosis of all cell types and axonal swellings (spheroids), and is typically observed 8–24 h following injury (24). Subacute PVL develops between 3–5 days following the insult, and is identified by focal tissue cavitation with macrophages in association with diffuse astro- and micro-gliosis in the surrounding white matter (24). Chronic PVL is identified by cystic cavitation or glial scar formation within weeks to months following the insult (24). In the control cases, there was no PVL, little or no reactive gliosis in the cerebral white matter and no significant pathological findings elsewhere in the brain.

Single-labeling immunocytochemistry

Samples of the frontal, parietal and/or occipital lobes were analyzed using antibodies presented in Table 1. Tissue was formalin-fixed and paraffin-embedded, and cut at 4 μm. To identify OLs and the myelin sheath of mature myelinating OLs, single-labeled immunocytochemistry (ICC) with the Olig2 and MBP antibodies were used, respectively (19). Although MBP is an indicator of mature myelinating OLs, it labels the myelin sheath and not the cell body, thereby making quantitation of the percentage of mature $Olig2^{+}/MBP^{+}$ OLs impossible. Of note, other antibodies such as CNPase, Rip, MOG, and PLP were also trialed for quantitation of mature OLs without success in our archival tissue. Activated microglia and reactive astrocytes were identified using the CD68 and the glial fibrillary acidic protein (GFAP) antibodies, respectively. Detection of apoptotic cells was performed utilizing the active caspase-3 antibody (technical and tissue limitations prevented the specific identification of these apoptotic cells). Of note, both TUNEL and *in situ* end labeling techniques were attempted for identification of apoptosis but without successful or replicable results. For all ICC experiments, microwave techniques (10 mM citrate buffer for 10–20 minutes) were used to enhance antigenicity, and primary antibodies were diluted in blocking buffer (phosphate-buffered saline/5% goat serum/ 0.1% Triton-X) and incubated overnight at 4°C. Staining was visualized with the chromagen 3,3′-diaminobenzidine. A light methyl green or haematoxylin counterstain was applied to each section. Negative control sections omitted the primary antibodies.

Double-labeling immunostaining in formalin-fixed and paraffin-embedded tissue

To determine the specificity of the Olig2 antibody in our tissue, double-labeling ICC or immunofluorescence was performed in four PVL and four control cases. The antibodies used in conjunction with Olig2 (1:20 000) were as follows: Adenomatous Polyposis Coli (APC), CD68, GFAP, vimentin (a marker of immature astrocytes), microtubule associated protein-2 (a neuronal marker) and tomato lectin (a marker of resting and activated microglia). The nuclear marker, DAPI (0.5 μg/mL), was used in all experiments. Specificities of each antibody were confirmed by processing control sections without primary antibodies.

Assessment of proliferating cells

To determine the density of proliferating cells, single-labeled ICC was performed using the Ki67 antibody. To identify proliferating cells, the Ki67 antibody was incubated with Olig2, GFAP and/or tomato lectin. Quantitation of the number of proliferating cells that were oligodendrocytes, astrocytes and/or microglia was not performed.

Quantitation of Olig2 density

To quantify Olig2 density in PVL and control tissue, the Neurolucida software program was used which utilizes a motorized x-y stage (MicroBrightField, VT, USA). The spatial

distribution of OL cell density was determined with two-dimensional graphic plots. At low magnification (20×), the boundaries of the cerebral cortex, white matter, ventricular border and necrotic periventricular foci were outlined. Because we were interested in the relationship between OL cell density and anatomical location of the OLs relative to the necrotic foci, a grid system was used. This system consisted of a grid with six squares (where possible), each 1 mm^2, which was placed over the section using the Neurolucida program. In the PVL cases, the first box was placed within the focal periventricular necrosis, with subsequent squares stepping away from it (Figure 1). The grid system was used in multiple tangents with no significant difference found in Olig2 cell density between tangents. For the control cases, the grid(s) were placed in the periventricular white matter in the same region as the typical necrotic foci in PVL (Figure 1). In addition, for both PVL and control cases, an analysis with the grid system was used in the intragyral white matter, that is, the most distant spatially from the necrotic periventricular foci (Figure 1). Cell counting was performed at 200× and the same counting technique was applied to tissue sections stained with Ki67 and caspase-3.

Quantitation of MBP, CD68 and GFAP

To assess the degree of MBP staining, a semiquantitative score was given based on staining intensity and distribution. The degree of MBP staining was assessed at 400× magnification and given a score of 0–3. A 2-year old control case with histologically “mature” myelin was arbitrarily given the score of 3 and was used as the standard reference for comparison; in this case, myelin was visible to the naked eye and was dark and dense; a Grade 0 = no MBP staining; Grade ½ = scattered MBP-positive axonal segments detected with the light microscope; Grade 1 = scattered but more prevalent fragments of MBP staining detected with the light microscope; Grade 2 = light staining visible to the naked eye that is less than a grade 3. This grading system is a modification of the one used previously by us (8,25). We also counted the number of OLs that expressed MBP immunostaining in the perikaryon in the central white matter of both PVL and control cases.

A semiquantitative scale identical to one previously published by us (19) was used to assess the density of CD68 and GFAP immunopositive cells. The highest number of immunopositive cells per high power field (hpf) at 400× magnification (0.173 mm^2) were counted following a survey of all fields. The grading system was as follows: Grade 0 = no cell staining; Grade ½ = scattered immunopositive cells/hpf; Grade 1 = 2–10 immunopositive cells/hpf; Grade 2 = 11–20 immunopositive cells/hpf; Grade 3 = >20 immunopositive cells/hpf.

Morphologic assessment of $O4^+$ OLs

To determine the morphology of developing OLs, the antibody against O4 (gift from Dr Steven Pfeiffer) was used in free-floating tissue that was fixed in 4% paraformaldehyde and cut at 40–50 μm. Six PVL and four control cases were studied. To visualize the O4 immunostaining, a μ-chain-specific fluorescein-conjugated IgM secondary antibody was used as previously described (19).

Statistical analysis for demographics

To compare gestational, post-natal and post-conceptional ages (PCA), as well as post-mortem intervals, between PVL and control cases, *t*-tests were used. A Fisher exact test was utilized to compare the gender distributions. Analysis of covariance (ANCOVA) was used to compare brain weight between PVL and control cases, adjusting for age.

Statistical analysis for Olig2, Ki67 and caspase-3 cell densities

Analysis is described for Olig2, but analysis of Ki67 and caspase-3 data was identical. To test the hypothesis that there is a reduction in Olig2 cell density in PVL cases compared with

controls, two analyses were performed, in which the outcome was Olig2, with diagnosis as the main predictor. These models also controlled for age. The first model was a doubly repeated measures ANCOVA, fit with the assumptions that (i) boxes within the same tangent and (ii) different tangents in the same case may be correlated. The interaction between age and diagnosis were also included in these models when significant. To test the hypothesis that Olig2 cell density increases with distance from the necrotic periventricular foci in PVL cases, we performed the same analysis but box by box. A repeated measures regression analysis of box number on cell density was also performed, assuming that tangents within the same case may be correlated. These analyses also controlled for age, brain region, the interaction between brain region and box number, histopathological age of the PVL lesion and the interaction between PVL histopathologic age and box number, if significant.

To test for differences between histopathological ages in PVL cases, repeated measures ANCOVA was used, controlling for age. First this analysis was performed using all boxes and then it was repeated only for Box 1 (at the necrotic foci). Repeated measures ANCOVA, controlling for age, was also used to test for differences between PVL and control cases in the intragyral region, and for differences between the intragyral region and other regions in both PVL and control cases (separately). Finally, repeated measures regression analyses were performed to test the effect of postmortem interval (PMI) on cell number and density. Interactions between PMI and diagnosis and intragyral/non-intragyral regions were considered as well.

Statistical analysis for CD68, GFAP and MBP scores

ANCOVA was used to test for differences between PVL and control cases in CD68 and GFAP in diffuse white matter and MBP staining in the central white matter, controlling for age (with a quadratic term for age, when significant). Paired Wilcoxon tests were performed to test for differences in CD68 and GFAP cell density between the focal and diffuse components of PVL, and between the diffuse white matter and the cerebral cortex in these same cases. ANCOVA was used to test for differences between brain regions in MBP staining, controlling for age. All data are presented as the mean ± SEM. A *P*-value of less than 0.05 was considered significant.

RESULTS

Clinical database

A total of 18 PVL and 18 control cases were analyzed in this study. The PCA range for the PVL cases was 29–95, with a median age of 39 PC weeks. For controls, the age range was 20–144 PC weeks, with a median age of 36 PC weeks. The mean gestational age (GA) (PVL: 34.5 ± 1.1 weeks; control: 33.6 ± 1.7 weeks), post-natal age (PVL: 7.0 ± 3.5 weeks; control: 9.9 ± 6.3 weeks) and PCA (PVL: 41.5 ± 3.5 weeks; control: 43.6 ± 7.0 weeks) did not differ significantly between the two groups. Total mean brain weight adjusted for age did not differ between the two groups (PVL: 304.9 ± 21.5 g; control: 343.7 ± 19.6 g; values adjusted for PCA), nor did PMI (PVL: 19.1 ± 5.7 h, range: 2–89 h; control: 16.8 ± 3.1 h, range: 1.5–48 h). Moreover, the different lengths of PMI did not appear to produce autolytic changes that visually affected the immunostaining patterns for any of the antibodies studied.

Neuropathology of cases examined

Of the 18 PVL cases examined, seven had acute foci of periventricular necrosis, 10 cases had subacute necrotic foci, and six cases had chronic foci with cavitation. There was one case with acute PVL only, three cases with subacute PVL only, and one case with chronic PVL only. The remaining 13 cases (72%) had a combination of two or all three of the histopathologic stages of PVL. Therefore, a total of 43 necrotic foci were examined, with 15 of them classified

as acute, 15 as subacute, and 13 as chronic. All analyses treated the histopathological age of the necrotic foci as a factor; however, because there was no difference between acute, subacute and chronic necrotic foci for the majority of the parameters examined, the data were combined, unless stated otherwise. For the majority of necrotic foci examined, the diameter rarely exceeded 1 mm, and thus could be considered "microcysts". The finding of "microcysts" is more prevalent today compared with the larger cysts observed in the past and hence are more difficult to identify by imaging techniques. The mean density of activated microglia in the white matter surrounding the necrotic foci in the PVL cases (2.35 ± 0.20 cells/hpf) was significantly higher than that of controls (1.42 ± 0.19 cells/hpf) ($P = 0.003$). Similarly, there was diffuse astrogliosis with the mean density of GFAP-positive astrocytes being 2.47 ± 0.18 cells/hpf in the PVL cases compared with 1.45 ± 0.18 cells/hpf in the controls ($P < 0.001$).

Specificity of Olig2 for oligodendrocytes

No double-labeling of Olig2 with any of the selected markers, except the cytoplasmic mature OL marker APC, was observed in the central or periventricular white matter or in the germinal matrix for either PVL or control cases (Figure 2).

Olig2 cell density in PVL cases vs. controls

Visual assessment of Olig2 cell density by light microscopy revealed no obvious difference between the PVL and control cases (Figure 3). In PVL cases, the Olig2 antibody did not appear to label apoptotic cells (ie, fragmented nuclei) within the periventricular necrotic foci or in the surrounding white matter, that is, similar staining patterns were observed for both PVL and control cases. Quantitative analysis of total Olig2 cell density (all six boxes combined), showed no significant difference between PVL (regardless of histopathological age of the lesion) and control cases, adjusting for age (Figure 4). As with the controls, there was a significant reduction in Olig2 cell density with increasing GA (and not PNA or PCA) in the PVL cases (data not shown) ($P = 0.02$). No effect of gender on Olig2 cell density in PVL or control cases was found (data not shown).

To test the hypothesis that the putative reduction in Olig2 cell density is greatest in the most severely damaged areas in PVL, we analyzed Olig2 cell density on a box-by-box basis. In contrast to the expected observation of decreased Olig2 cell density around the necrotic focus, we found a significant increase in Olig2 density in this area (Box 1) compared with more distant areas (Box 6) ($P = 0.003$) (Table 2). This preservation of Olig2 cell density within the necrotic "core" occurred in regions where there was axonal injury as evidenced by the presence of spheroids, and occurred for all histopathological stages examined. Previously, we reported that the intragyral (distant) white matter in PVL is relatively spared of gliosis, suggesting that the brunt of the white matter injury is in the deep white matter (19). We found, however, no significant difference in Olig2 cell density between the periventricular (127.9 ± 11.7 cells/mm^2) and the intragyral white matter (115.8 ± 12.9 cells/mm^2) in the PVL cases (P = NS). In addition, no significant difference was found in the intragyral Olig2 cell density between PVL and control cases (data not shown).

Caspase-3 as a marker of apoptosis in PVL

Analysis of caspase-3 cell density revealed no significant difference between PVL (6.8 ± 2.5 cells/mm^2) and control cases (2.1 ± 2.6 cells/mm^2) in the periventricular white matter (P = 0.21), despite two PVL cases that were "outliers" (24.9 ± 6.3 cells/mm^2). Of note, the mean caspase-3 cell density in the PVL cases was 2.3 ± 0.9 cells/mm^2 without the outliers. Analysis of caspase-3 cell density on a box-by-box basis, however, revealed that there was a significantly greater density within the necrotic foci (Box 1: 9.6 ± 2.1 cells/mm^2) compared with distant areas (Box 6: 2.0 ± 1.2 cells/mm^2) ($P = 0.001$), and compared with the relative non-necrotic site in controls (Box 1: 0.9 ± 2.2 cells/mm^2) ($P = 0.01$). We were unable to identify the cell

type of the caspase-3 immunopositive cells. We found, however, no correlation between the density of Olig2 cells and caspase-3 immunopositive cells on a box-by-box basis in PVL cases (data not shown), suggesting that if Olig2 cell death was occurring, the dying Olig2 cells were being replenished by inward migration and/or proliferation of OL precursors ($NG2^+$, $PDGFR^+$).

Proliferation in PVL and controls

Proliferating cells in both the periventricular necrotic focus (Box 1) and more distant "spared" areas (Box 6) in PVL cases, and in the comparable region in controls, were identified as OLs ($Olig2^+$) and microglia, but not astrocytes (data not shown). In addition, these cells, based on morphological assessment, did not appear apoptotic. Analysis in the periventricular white matter (all 6 boxes) showed that while there appeared to be a higher density of proliferating cells in the PVL cases (7.7 ± 2.1 cells/mm^2) compared with age-adjusted controls (6.4 ± 2.0 cells/mm^2), this was not significant (P = NS). There was also no significant difference in proliferating cell density in PVL cases when analyzing boxes from within (Box 1) and progressing away from the necrotic foci, that is, the density of proliferating cells in Box 1 (7.46 ± 2.03 cells/mm^2) was not significantly different to Box 6, the most distant area from the necrotic foci analysed (7.07 ± 1.87 cells/mm^2). No significant difference in Ki67 cell density was found between PVL (3.1 ± 1.2 cells/mm^2) and controls (4.6 ± 1.1 cells/mm^2) in the intragyral white matter. There was no effect of age on the density of proliferating cells in PVL cases (data not shown).

MBP staining patterns

Little or no MBP immunostaining in the central white matter in PVL cases less than 30 PC weeks (n = 2) or in control cases less than 35 PC weeks (n = 8) was found, supporting previous observations. By 40 PC weeks, however, nearly all cases examined in this dataset had some degree of myelin [PVL: n = 9/10 cases (90%); control: n = 8/9 cases (89%)], with the timing of appearance occurring first in the parietal white matter, followed by the occipital and then frontal white matter. We found no significant difference in the overall degree of MBP immunostaining in central white matter between PVL (0.74 ± 0.10) and control (0.79 ± 0.10) cases, adjusting for age. There was, however, a significant increase in MBP degree with increasing GA for both groups ($P < 0.0001$), consistent with the progression in myelination over time in both PVL and control cases (data not shown).

Despite similar age-related degrees of MBP immunostaining between PVL and control cases in the central cerebral white matter in association with maintained Olig2 cell density (Figure 5), we observed striking qualitative abnormalities in the patterns of myelin staining in the PVL cases. First, there was an increased number of OLs expressing MBP in the perikaryon in the diffuse component of PVL cases (5.20 ± 0.53 cells) compared with controls (0.00 ± 0.00 cells) ($P < 0.0001$) (Figure 6). Additionally, we observed abnormal MBP immunostaining within the organizing and chronic necrotic foci, in association with axonal injury (spheroids) and maintained Olig2 cell density. In many instances, the degree of MBP immunostaining was intensely present in the necrotic foci, in contrast to the lack of MBP expected for age in the surrounding diffuse white matter (8,25) (Figure 7). Of the 43 necrotic foci examined, there was no abnormal MBP immunostaining in the acutely necrotic foci (n = 0/15), while abnormal MBP immunostaining was present in 73% of subacute PVL foci (n = 11/15) and in 62% of chronic PVL foci (n = 8/15).

O4 cell morphology

In two of the six cases of PVL analyzed, we found O4-positive OL soma without processes (Figure 8). Of the four controls studied, no abnormalities in OL-process morphology were noted (Figure 8).

DISCUSSION

It has long been postulated that hypomyelination in PVL is caused by lethal injury to preOLs and subsequent reduction in mature myelinating OLs (18,38,41,49). Nevertheless, verification of this hypothesis by a systematic quantitative analysis of OLs in a large dataset of PVL cases at all histopathologic stages and in conjunction with MBP assessment, has been lacking. Using the antibody to Olig2, a transcription factor expressed throughout the entire OL lineage, we did not find the postulated reduction in total OL cell density in PVL cases compared with age-related controls. Despite the "maintenance" of total OL density in the 18 PVL cases in our series, however, we found abnormalities of O4 and MBP immunostaining, with a loss of OL cell processes in some PVL cases, an increase and persistence of OLs with perikaryal (as opposed to distal cytoplasmic process) MBP immunostaining in the diffusely damaged, pre-myelinated white matter and abnormal MBP expression in the periventricular necrotic foci. These findings provide new insight into the potential mechanisms underlying the myelin deficits observed by neuroimaging in survivors of prematurity with PVL.

This study is based upon the use of the Olig2 antibody to identify OLs. Functional studies in *Olig2*-null mice show that these mice entirely lack preOLs in the spinal cord, and have reduced preOLs in the forebrain (30). The *Olig1/2* double knockout, however, demonstrates a completely ablated preOL and spinal motor neuron phenotype, suggesting that these genes "couple" glial and neuronal subtype differentiation (52). Recently, it has been suggested that Olig2 is also involved in the development of astrocytes in the rodent forebrain (34,44) and spinal cord (35), and in neuronal specification, but not astrocyte development in the human cerebral cortex (23). To ensure the specificity of the Olig2 antibody in our forebrain samples, we performed a battery of double-labeled immunocytochemical studies with Olig2 and other cell type markers. We found no co-localization of Olig2 with microglia, astrocytes or neurons, in either the central white matter or in the germinal matrix, the highly proliferative area where one would expect the earliest OL progenitors. Olig2, however, co-localized with the mature OL cytoplasmic marker, APC. Thus, the Olig2 antibody used in this study specifically labels OLs in the developing human cerebral white matter during the time frame of our analysis. The differences between our results and those of others showing Olig2 co-localization with other cell types (23,34,44) are likely caused by differences in species (34,44), antibody source, methodology and developmental stages examined in the human fetus [mid-late gestation in our study vs. early gestation (8–22 PC weeks)] (23).

Our major finding is that Olig2 cell density is not reduced in the focal and/or diffuse components of PVL compared with controls adjusted for age. Moreover, there is no difference in Olig2 cell density among acute, subacute and/or chronic stages of PVL, suggesting that Olig2 cells do not progressively die over the temporal evolution of the white matter damage. We also found an increase in Olig2 cell density in areas within and immediately adjacent to the necrotic foci (regardless of histopathological age) compared with areas 4–6 mm distant from them. It is possible that a loss of white matter tissue, perhaps caused by anterograde or retrograde destruction of axons passing through sites of necrosis, with associated loss in Olig2 cell number maintains the same Olig2 cell density in PVL cases as in controls. Such "tissue collapse", however, is not usually present in acute or early subacute lesions, but only in chronic foci of necrosis. Therefore, the finding of similar Olig2 cell densities between the different histopathological stages of PVL and controls, suggests that there was minimal tissue loss in our PVL cases. There was also no difference in overall brain weight between the PVL and control cases in this study, again arguing against the possibility of substantial loss of cerebral white matter volume (and area) in our PVL cases. In this regard, neuroimaging studies in premature infants dying around term-equivalent, as in this autopsy study, do not show volume loss of *unmyelinated* white matter in the cerebrum (22). Thus, it is unlikely that a concomitant

loss of white matter volume masks a substantial loss of Olig2 cells in the PVL cases in this study.

Our data raise the possibility that OL progenitor ($NG2^+$, $PDGFR^+$) proliferation is triggered to generate new OLs, thereby compensating for a "masked" OL cell loss in PVL that occurred hyper-acutely, prior to the time-periods "captured" in our histological sections. Oligodendrocytes are known to proliferate in response to multiple insults, including hypoxia-ischemia, at all ages (5,7,9,15,31,33,46,51). With an antibody to Ki67, we found that OLs, as well as microglia, proliferate in the focal and diffuse components of PVL. Nevertheless, while there was a trend for increased density of Ki67-immunolabeled cells in PVL, the difference was not significantly different from control cases. This latter result is surprising given the significant increase in activated microglial cell density in the PVL cases compared with controls in this and other studies by us (19), an observation presumed to be caused by, at least in part, microglial proliferation. It is possible, however, that we are "missing" the peak timing of microglial proliferation after the insult in our cases, as microglial hyperplasia occurs almost immediately (within hours) after hypoxic-ischemic injury in neonatal rodent brain (51), and virtually all of our cases have evidence of older injury, that is, subacute and/or chronic focal lesions, combined with acute lesions. The 40% increase of reactive microglia within PVL may also be caused by rapid recruitment and migration from blood or the subventricular zone, rather than cell division *in situ*.

The lack of significantly increased Ki67 cell density in PVL cases suggests the possibility that we are also "missing" the peak period of OL proliferation following injury. It also suggests the possibility that the maintenance of Olig2 cell density overall, and the increased cell density at the necrotic focus in particular, is caused by OL migration from the site of OL progenitors, that is, the subventricular zone of the lateral ventricle, perhaps after a hyperacute loss or injury of preOLs prior to detection in our autopsy series of PVL cases. In response to hypoxic-ischemic injury in the neonatal (5,26,45,51) and adult rodent (33,46), and in models of multiple sclerosis (37,40), OL progenitors migrate toward the site of injury presumably in an attempt to repair, and this can occur within hours following injury (26,45). Moreover, OL progenitors are depleted in the subventricular zone within hours of hypoxicischemic injury in the perinatal rat model (26,45), suggesting that their outward migration results in subventricular depletion. In experimental autoimmune encephalomyelitis, subventricular OL progenitor cells undergo "oligodendrogliosis", thereby contributing new OLs to demyelinated areas (40). Our finding of increased Olig2 cell density at the necrotic focus is possibly caused by NG2-positive OLs that are unable to mature to a myelin-forming phenotype, an avenue for future study.

The question arises: what is causing the myelin deficits in survivors of PVL? We suggest: (i) inadequate repair involving proliferation and migration of OL progenitors to the necrotic core; (ii) an arrest in maturation of the OL progenitor or preOL to the mature phenotype; (iii) an inability of the mature OL to produce or traffic sufficient myelin; and/or (iv) primary axonal injury with defective axonal signaling for myelin initiation and production by OLs (Figure 9). The observation of increased OLs expressing MBP directly in the perikaryon, rather than on the processes, in the PVL cases supports dysregulation in MBP mRNA trafficking and/or dysfunction of myelin sheath wrapping. During the process of myelin sheath formation, MBP mRNA translocates from the OL cell body (perikaryon) to the distal cytoplasmic processes that eventually undergo wrapping and membrane compaction to form the myelin sheath (4, 10,39,47,48). Recently, N-methyl-D-aspartate receptors, a mediator of preOL excitotoxicity (36,43), have been reported on the processes and not somata of preOLs, and can rapidly detach and disintegrate following ischemia in a murine model (43). In PVL, a similar damage may occur to distal processes but not necessarily cell number, as reflected by our initial O4 immunostaining results, in which the preOL soma is preserved but the cell processes have disintegrated. In regards to defective axonal-OL signaling, we found axonal damage occurs in

the periventricular necrotic foci, as reported in previous studies and we have recently identified that widespread axonal injury also occurs in PVL (unpublished observations). In our PVL cases, the prominence of Olig2 cells and MBP-positive fragments in the necrotic foci suggest that the mature OLs may attempt to produce myelin, but the process is abnormal without intact axons to signal the proper timing and formation of myelin sheaths. Using an ischemic mouse model, Mandai et al (33), demonstrated that early axonal disruption occurs prior to changes in PLP mRNA, suggesting that the damage to axons precedes that of damage to OLs and myelin (33). Our finding of abnormal MBP immunostaining within the necrotic foci was not reported in a previous study examining myelination and OLs in PVL (20). Given that the average age of the cases studied by Iida et al. (20) was approximately 15 weeks older than those used in the present study, this age difference is likely enough to have affected myelination patterns.

In conclusion, this study indicates that myelin abnormalities and, in some instances, loss of preOL cell processes occur in PVL without a loss of OL cell density. Our findings raise the intriguing possibility that a hyperacute loss of preOLs is replenished, by proliferation and migration of OL progenitors from subventricular zones, a process that may not always be adequate and thereby result in neurological disability. They also suggest that the deficits in myelination are caused by loss of OL-cytoplasmic processes and defective MBP trafficking, perhaps secondary to process loss. This study highlights the need to analyze in greater depth the potential factors critical for OL proliferation, migration and repair for optimal myelination in long-term survivors of PVL as crucial leads for the development of successful therapeutic strategies in PVL.

Acknowledgments

We appreciate the help of Ms Sarah E. Andiman for technical assistance and illustrations, Mr Richard Belliveau for formatting assistance and of Ms Lena L. Liu in histological preparations. We also thank Dr Chuck Stiles (Dana Farber Cancer Institute, Harvard Medical School, MA) for the Olig2 antibody and Dr Steven Pfeiffer (University of Connecticut Health Center, Farmington, CT) for the O4 antibody.

Grant sponsors: National Institute of Neurological Disorders and Stroke (NINDS), PO1-NS38475; National Institute of Child Health and Development (NICHD), P30-HD18655 (Children's Hospital Boston Developmental Disabilities Center); National Multiple Sclerosis Society.

REFERENCES

1. Arai Y, Deguchi K, Mizuguchi M, Takashima S. Expression of beta-amyloid precursor protein in axons of periventricular leukomalacia brains. Pediatr Neurol 1995;13:161–163. [PubMed: 8534283]
2. Arnett HA, Fancy SP, Alberta JA, Zhao C, Plant SR, Kaing S, et al. bHLH transcription factor Olig1 is required to repair demyelinated lesions in the CNS. Science 2004;306:2111–2115. [PubMed: 15604411]
3. Back SA, Luo NL, Borenstein NS, Levine JM, Volpe JJ, Kinney HC. Late oligodendrocyte progenitors coincide with the developmental window of vulnerability for human perinatal white matter injury. J Neurosci 2001;21:1302–1312. [PubMed: 11160401]
4. Back SA, Luo NL, Borenstein NS, Volpe JJ, Kinney HC. Arrested oligodendrocyte lineage progression during human cerebral white matter development: dissociation between the timing of progenitor differentiation and myelinogenesis. J Neuropathol Exp Neurol 2002;61:197–211. [PubMed: 11853021]
5. Back SA, Han BH, Luo NL, Chriction CA, Xanthoudakis S, Tam J, et al. Selective vulnerability of late oligodendrocyte progenitors to hypoxia-ischemia. J Neurosci 2002;22:455–463. [PubMed: 11784790]
6. Back SA, Luo NL, Mallinson RA, O'Malley JP, Wallen LD, Frein B, et al. Selective vulnerability of preterm white matter to oxidative damage defined by F2-isoprostanes. Ann Neurol 2005;58:108–120. [PubMed: 15984031]

7. Biran V, Joly LM, Heron A, Vernet A, Vega C, Mariani J, et al. Glial activation in white matter following ischemia in the neonatal P7 rat brain. Exp Neurol 2006;199:103–112. [PubMed: 16697370]
8. Brody BA, Kinney HC, Kloman AS, Gilles FH. Sequence of central nervous system myelination in human infancy. I. An autopsy study of myelination. J Neuropathol Exp Neurol 1987;46:283–301. [PubMed: 3559630]
9. Cao Y, Gunn AJ, Bennet L, Wu D, George S, Gluckman PD, et al. Insulin-like growth factor (IGF)-1 suppresses oligodendrocyte caspase-3 activation and increases glial proliferation after ischemia in near-term fetal sheep. J Cereb Blood Flow Metab 2003;23:739–747. [PubMed: 12796722]
10. Colman DR, Kreibich G, Frey AB, Sabatini DD. Synthesis and incorporation of myelin polypeptides into CNS myelin. J Cell Biol 1982;95:598–608. [PubMed: 6183276]
11. Counsell SJ, Allsop JM, Harrison MC, Larkman DJ, Kennea NL, Kapellou O, et al. Diffusion-weighted imaging of the brain in preterm infants with focal and diffuse white matter abnormality. Pediatrics 2003;112:1–7. [PubMed: 12837859]
12. Dammann O, Kuban KC, Leviton A. Perinatal infection, fetal inflammatory response, white matter damage, and cognitive limitations in children born preterm. Ment Retard Dev Disabil Res Rev 2002;8:46–50. [PubMed: 11921386]
13. De Vries LS, Connell JA, Dubowitz LM, Oozeer RC, Dubowitz D, Pennock JM. Neurological, electrophysiological and MRI abnormalities in infants with extensive cystic leukomalacia. Neuropediatrics 1987;18:61–66. [PubMed: 3600997]
14. Flodmark O, Lupton B, Li D, Stimac GK, Roland EH, Hill A, et al. MR imaging of periventricular leukomalacia in childhood. AJR Am J Roentgenol 1989;152:583–590. [PubMed: 2783813]
15. Glezer I, Lapointe A, Rivest S. Innate immunity triggers oligodendrocyte progenitor reactivity and confines damages to brain injuries. FASEB J 2006;20:750–752. [PubMed: 16464958]
16. Goncalves LF, Chaiworapongsa T, Romero R. Intrauterine infection and prematurity. Ment Retard Dev Disabil Res Rev 2002;8:3–13. [PubMed: 11921380]
17. Hagberg H, Peebles D, Mallard C. Models of white matter injury: comparison of infectious, hypoxic-ischemic, and excitotoxic insults. Ment Retard Dev Disabil Res Rev 2002;8:30–38. [PubMed: 11921384]
18. Haynes RL, Baud O, Li J, Kinney HC, Volpe JJ, Folkerth RD. Nitrosative and oxidative injury to premyelinating oligodendrocytes in periventricular leukomalacia. J Neuropathol Exp Neurol 2003;62:441–450. [PubMed: 12769184]
19. Haynes RL, Folkerth RD, Keefe RJ, Sung I, Swzeda LI, Rosenberg PA, et al. Oxidative and nitrative injury in periventricular leukomalacia: a review. Brain Pathol 2005;15:225–233. [PubMed: 16196389]
20. Iida K, Takashima S, Ueda K. Immunohistochemical study of myelination and oligodendrocyte in infants with periventricular leukomalacia. Pediatr Neurol 1995;13:296–304. [PubMed: 8771165]
21. Inder TE, Wells SJ, Mogridge NB, Spencer C, Volpe JJ. Defining the nature of the cerebral abnormalities in the premature infant: a qualitative magnetic resonance imaging study. J Pediatr 2003;143:171–179. [PubMed: 12970628]
22. Inder TE, Warfield SK, Wang H, Huppi PS, Volpe JJ. Abnormal cerebral structure is present at term in premature infants. Pediatrics 2005;115:286–294. [PubMed: 15687434]
23. Jakovcevski I, Zecevic N. Olig transcription factors are expressed in oligodendrocyte and neuronal cells in human fetal CNS. J Neurosci 2005;25:10064–10073. [PubMed: 16267213]
24. Kinney HC, Brody BA, Kloman AS, Gilles FH. Sequence of central nervous system myelination in human infancy. II. Patterns of myelination in autopsied infants. J Neuropathol Exp Neurol 1988;47:217–234. [PubMed: 3367155]
25. Kinney, HC.; Haynes, RL.; Folkerth, RD. White matter disorders in the perinatal period. In: Golden, JA.; Harding, B., editors. Pathology and Genetics: Acquired and Inherited Diseases of the Developing Nervous System. Basel: ISN Neuropathology Press; 2004. p. 29-40.
26. Levison SW, Rothstein RP, Romanko MJ, Synder MJ, Meyers RL, Vannucci SJ. Hypoxia/ischemia depletes the rat perinatal subventricular zone of oligodendrocyte progenitors and neural stem cells. Dev Neurosci 2001;23:234–247. [PubMed: 11598326]

27. Ligon KL, Alberta JA, Kho AT, Weiss J, Kwaan MR, Nutt CL, et al. The oligodendroglial lineage marker OLIG2 is universally expressed in diffuse gliomas. J Neuropathol Exp Neurol 2004;63:499–509. [PubMed: 15198128]
28. Ligon KL, Kesari S, Kitada M, Sun T, Amett HA, Alberta JA, et al. Development of NG2 neural progenitor cells requires Olig gene function. Proc Natl Acad Sci USA 2006;103:7853–7858. [PubMed: 16682644]
29. Lu QR, Yuk D, Alberta JA, Zhu Z, Pawlitzky I, Chan J, et al. Sonic hedgehog—regulated oligodendrocyte lineage genes encoding bHLH proteins in the mammalian central nervous system. Neuron 2000;25:317–329. [PubMed: 10719888]
30. Lu QR, Sun T, Zhu Z, Ma N, Garcia M, Stiles C, et al. Common developmental requirement for Olig function indicates a motor neuron/oligodendrocyte connection. Cell 2002;109:75–86. [PubMed: 11955448]
31. Ludwin SK. Proliferation of mature oligodendrocytes after trauma to the central nervous system. Nature 1984;308:274–275. [PubMed: 6700730]
32. Maalouf EF, Duggan PJ, Counsell SJ, Rutherford MA, Cowan F, Azzopardi D, et al. Comparison of findings on cranial ultrasound and magnetic resonance imaging in preterm infants. Pediatrics 2001;107:719–727. [PubMed: 11335750]
33. Mandai K, Matsumoto M, Kitagawa K, Matsushita K, Ohtsuki T, Mabuchi T, et al. Ischemic damage and subsequent proliferation of oligodendrocytes in focal cerebral ischemia. Neuroscience 1997;77:849–861. [PubMed: 9070757]
34. Marshall CA, Novitch BG, Goldman JE. Olig2 directs astrocyte and oligodendrocyte formation in postnatal subventricular zone cells. J Neurosci 2005;25:7289–7298. [PubMed: 16093378]
35. Masahira N, Takebayashi H, Ono K, Watanabe K, Ding L, Furusho M, et al. Olig2-positive progenitors in the embryonic spinal cord give rise not only to motoneurons and oligodendrocytes, but also to a subset of astrocytes and ependymal cells. Dev Biol 2006;293:358–369. [PubMed: 16581057]
36. Micu I, Jiang Q, Coderre E, Ridsdale A, Zhang L, Woulfe J, et al. NMDA receptors mediate calcium accumulation in myelin during chemical ischaemia. Nature 2006;439:988–992. [PubMed: 16372019]
37. Newcombe J, Eriksson B, Ottervald J, Yang Y, Frazen B. Extraction and proteomic analysis of proteins from normal and multiple sclerosis postmortem brain. J Chromatogr B Analyt Technol Biomed Life Sci 2005;815:191–202.
38. Oka A, Belliveau MJ, Rosenberg PA, Volpe JJ. Vulnerability of oligodendroglia to glutamate: pharmacology, mechanisms, and prevention. J Neurosci 1993;13:1441–1453. [PubMed: 8096541]
39. Pedraza L, Fidler L, Staugaitis SM, Colman DR. The active transport of myelin basic protein into the nucleus suggests a regulatory role in myelination. Neuron 1997;18:579–589. [PubMed: 9136767]
40. Picard-Riera N, Decker L, Delarasse C, Goude K, Nait-Oumesmar B, Liblau R, et al. Experimental autoimmune encephalomyelitis mobilizes neural progenitors from the subventricular zone to undergo oligodendrogenesis in adult mice. Proc Natl Acad Sci USA 2002;99:13211–13216. [PubMed: 12235363]
41. Rezaie P, Dean A. Periventricular leukomalacia, inflammation and white matter lesions within the developing nervous system. Neuropathology 2002;22:106–132. [PubMed: 12416551]
42. Rowitch DH, Lu QR, Kessaris N, Richardson WD. An “oligarchy” rules neural development. Trends Neurosci 2002;25:417–422. [PubMed: 12127759]
43. Salter MG, Fern R. NMDA receptors are expressed in developing oligodendrocyte processes and mediate injury. Nature 2005;438:1167–1171. [PubMed: 16372012]
44. Setoguchi T, Kondo T. Nuclear export of OLIG2 in neural stem cells is essential for ciliary neurotrophic factor-induced astrocyte differentiation. J Cell Biol 2004;166:963–968. [PubMed: 15452140]
45. Skoff RP, Bessert DA, Barks JD, Song D, Cerghet M, Silverstein FS. Hypoxic-ischemic injury results in acute disruption of myelin gene expression and death of oligodendroglial precursors in neonatal mice. Int J Dev Neurosci 2001;19:197–208. [PubMed: 11255033]
46. Tanaka K, Nogawa S, Suzuki S, Dembo T, Kosakai A. Upregulation of oligodendrocyte progenitor cells associated with restoration of mature oligodendrocytes and myelination in peri-infarct area in the rat brain. Brain Res 2003;989:172–179. [PubMed: 14556938]

47. Trapp BD, Moench T, Pulley M, Barbosa E, Tennekoon G, Griffin J. Spatial segregation of mRNA encoding myelin-specific proteins. Proc Natl Acad Sci USA 1987;84:7773–7777. [PubMed: 3478726]

48. Verity AN, Campagnoni AT. Regional expression of myelin protein genes in the developing mouse brain: in situ hybridization studies. J Neurosci Res 1988;21:238–248. [PubMed: 2464076]

49. Volpe JJ. Neurobiology of periventricular leukomalacia in the premature infant. Pediatr Res 2001;50:553–562. [PubMed: 11641446]

50. Yoon BH, Park CW, Chaiworapongsa T. Intrauterine infection and the development of cerebral palsy. BJOG 2003;110:124–127. [PubMed: 12763129]

51. Zaidi AU, Bessert DA, Ong JE, Xu H, Barks JD, Silverstein FS, et al. New oligodendrocytes are generated after neonatal hypoxic-ischemic brain injury in rodents. Glia 2004;46:380–390. [PubMed: 15095368]

52. Zhou Q, Anderson DJ. The bHLH transcription factors OLIG2 and OLIG1 couple neuronal and glial subtype specification. Cell 2002;109:61–73. [PubMed: 11955447]

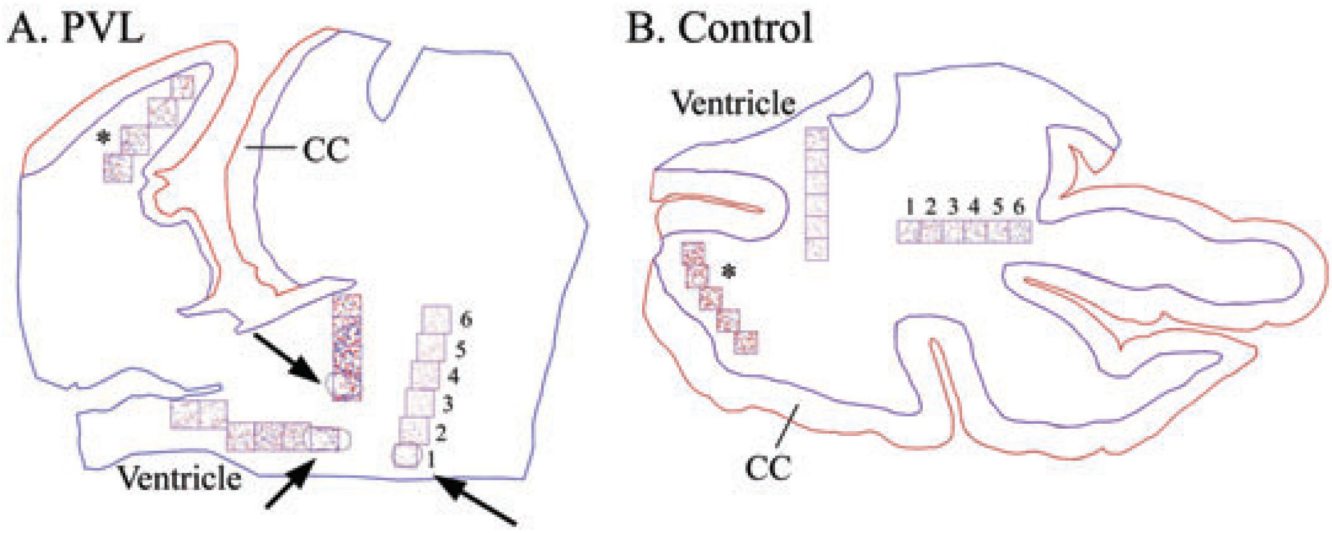

Figure 1.

Neurolucida images of Olig2 cell density analysis in a 40 post-conceptional (PC) week periventricular leukomalacia (PVL) case (**A**) and a 40 PC week control case (**B**) (identical counting methods were used for caspase-3 and Ki67). At low power (20×) the boundaries of the white matter (in blue) and the cerebral cortex (CC) (in red) were outlined. A boundary was then drawn around each necrotic focus (arrows; **A**). Using a grid system of six 1 mm^2 boxes (where possible), with the first box placed over the PVL focus and subsequent boxes progressing away from it, Olig2-immunopositive cells were counted using pre-selected markers (at 200×). If more than one necrotic focus was found within each tissue section, a separate analysis was performed, hence the different markers used for each grid system. Analysis of Olig2 cell density was also performed in the distant intragyral white matter (*).

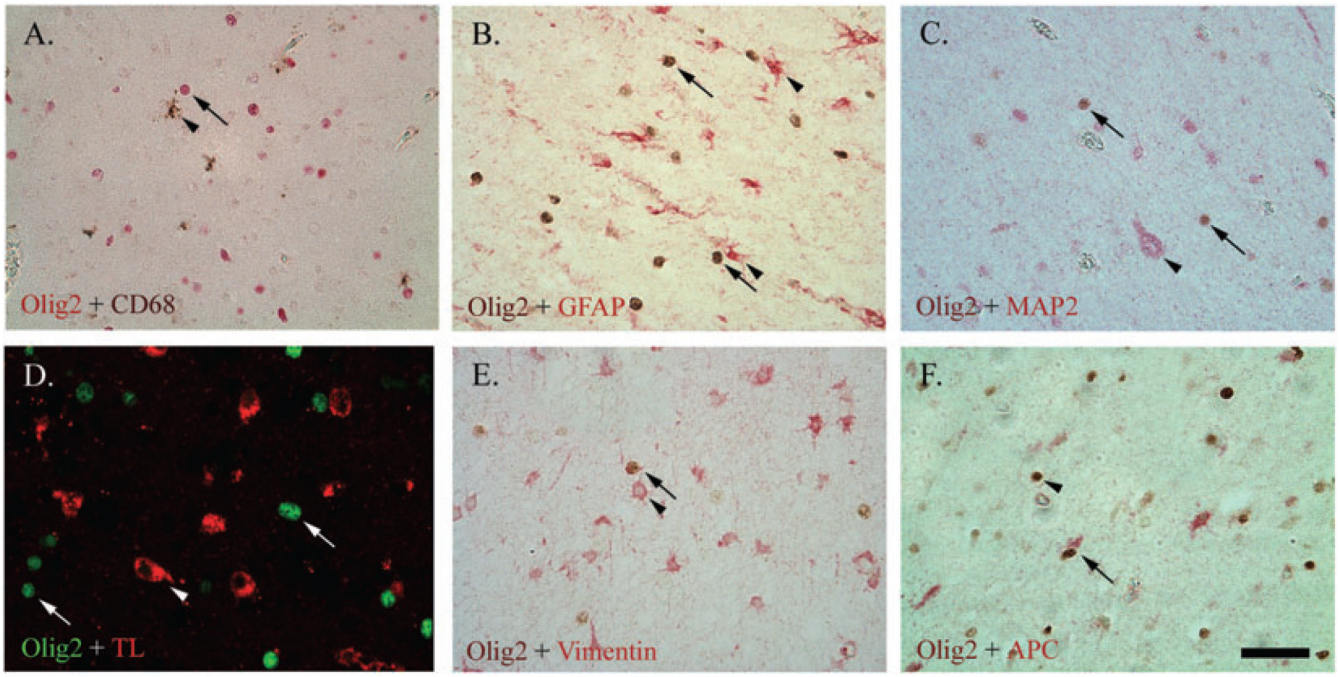

Figure 2.

Double-labeling of Olig2 (nuclear) with the microglial markers CD68 (brown; **A**) and tomato lectin (TL, red; **D**), glial fibrillary acidic protein (GFAP)-positive astrocytes (red; **B**), microtubule associated protein-2 (MAP-2)-positive neurons (red; **C**), and vimentin-positive immature astrocytes (red; **E**), showed no co-localization. There was co-localization, however, between Olig2 and the mature oligodendrocyte lineage (OL) marker Adenomatous Polyposis Coli (APC) (red; **F**). For images **A**–**E**, arrows indicate Olig2 and arrow heads indicate other markers. For image **F**, the arrow indicates the mature OL (Olig2+/APC+), whereas the arrowhead indicates the immature OL (Olig2+/APC−). All images are at 400× magnification. Scale bar = 50 μm.

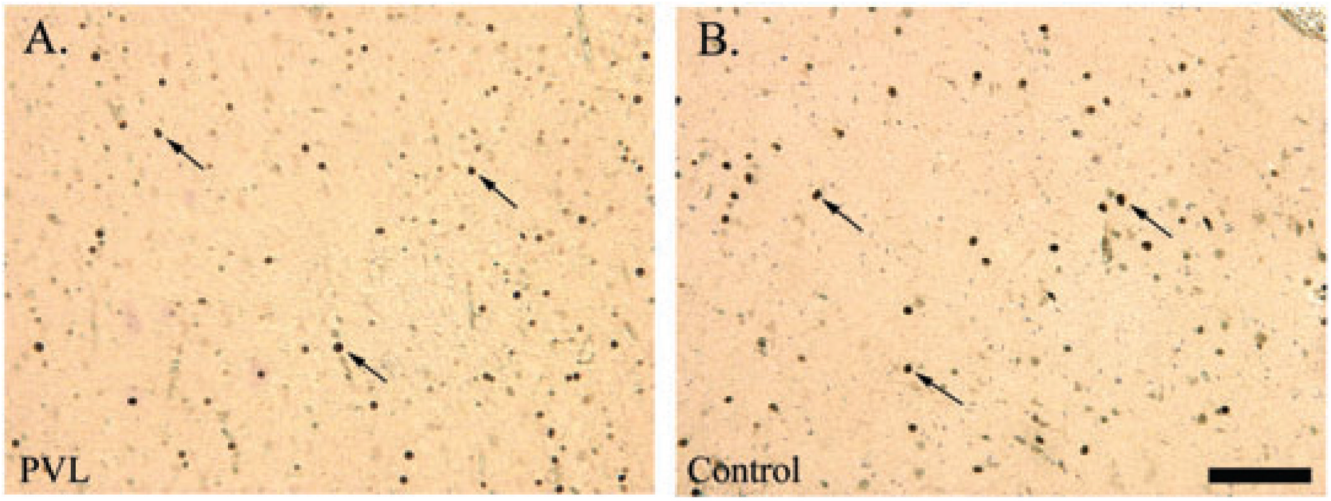

Figure 3.
Olig2 immunostaining (arrows) of nuclei in the diffuse white matter of a 39 post-conceptional (PC) week periventricular leukomalacia (PVL) case (**A**) and a 35 PC week control case (**B**). Images are at 200× magnification. Scale bar = 100 μm.

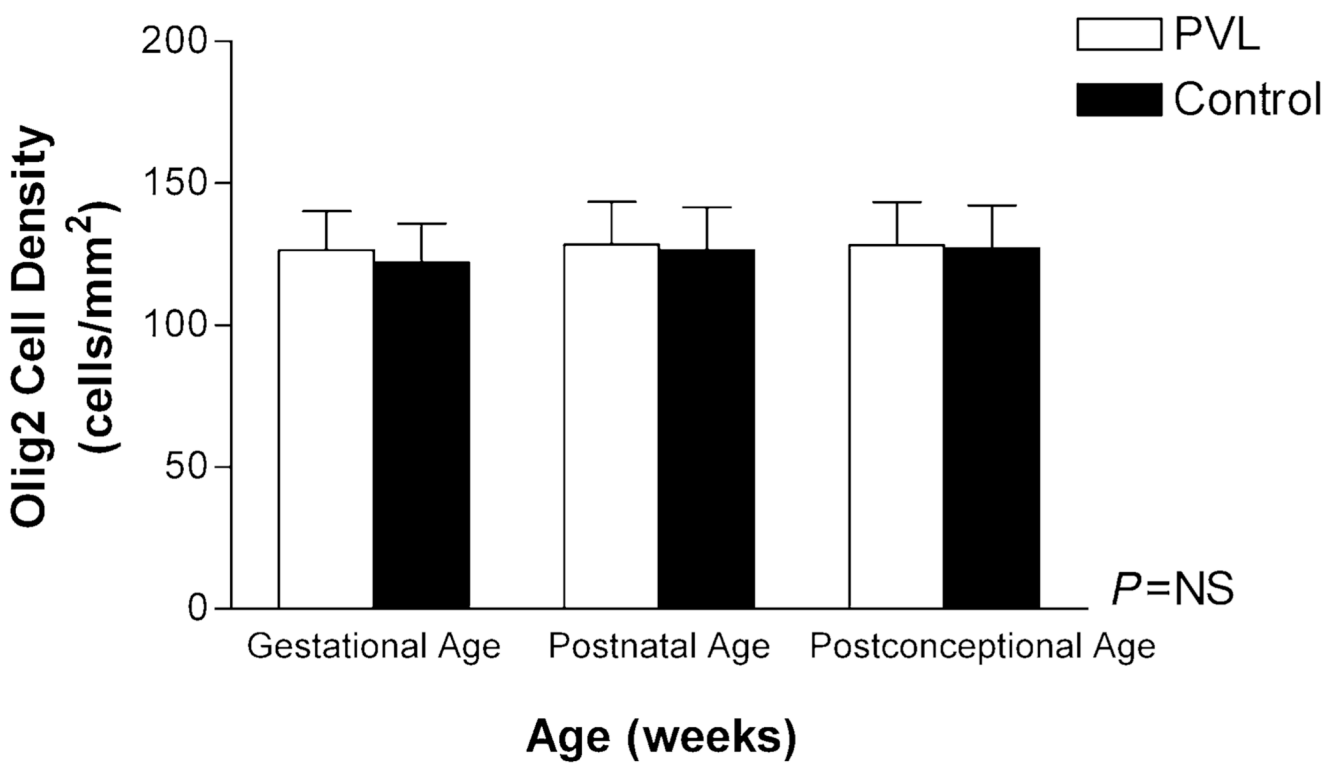

Figure 4.
Olig2 cell density (cells/mm^2) (all six boxes), was not different between periventricular leukomalacia (PVL) (n = 18) and control cases (n = 18) adjusting for gestational, post-natal and post-conceptional age. Abbreviation: NS = not significant.

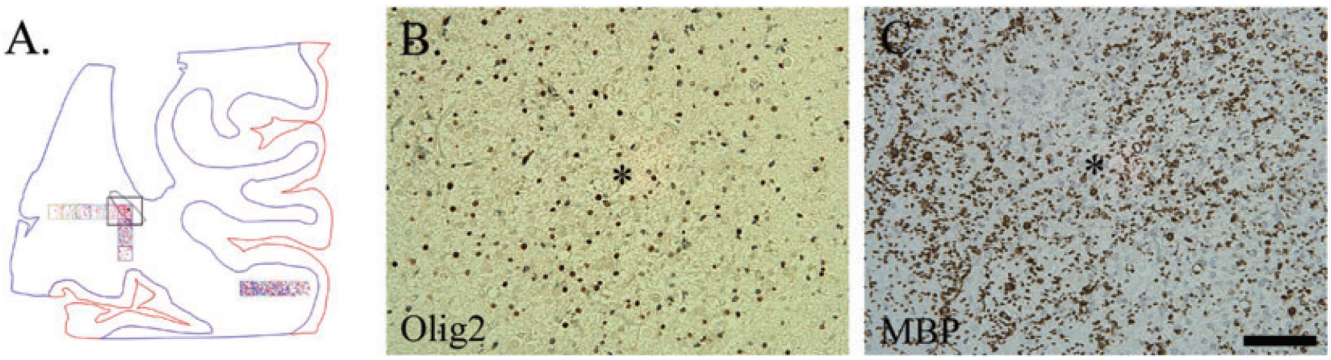

Figure 5.

A. Neurolucida image of Case 14 (44 post-conceptional weeks) with a subacute (organizing) necrotic focus (*) located in the optic radiation (highlighted by the black outlined box). Olig2 (**B**) and myelin basic protein (**C**) immunostaining were detected within this necrotic focus (*). Images are at 200× magnification. Scale bar = 100 μm.

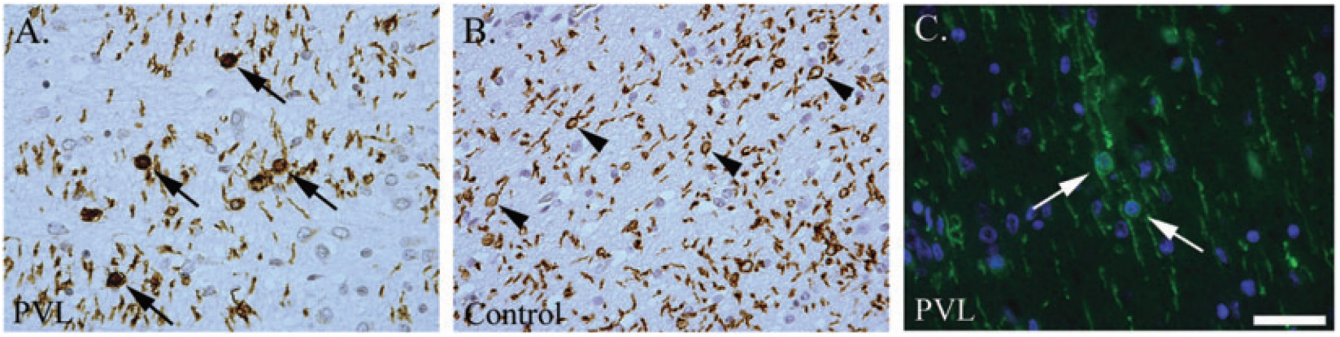

Figure 6.

Increased number of oligodendrocytes (OLs) (observed qualitatively) with myelin basic protein (MBP) immunostaining in the perikaryon (arrows) in periventricular leukomalacia (PVL) cases (**A**) compared with controls (**B**) which had more MBP-positive tubules (arrowheads). Double-labeling immunofluorescence with MBP (green) and the nuclear marker DAPI (blue) show perikaryl MBP immunostaining (arrows). Images are at 400× magnification. Scale bar = 50 μm.

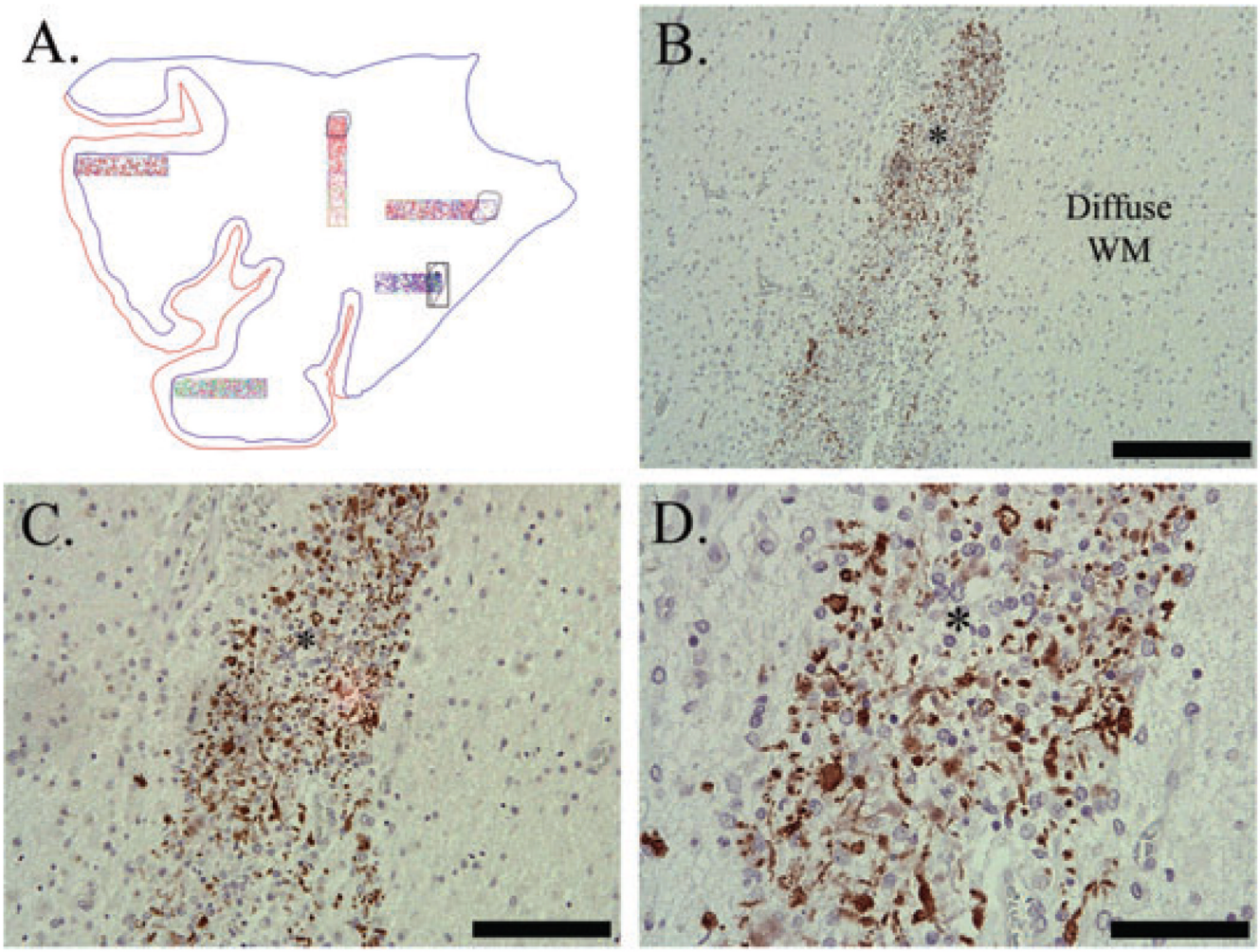

Figure 7.
Abnormal myelin basic protein (MBP) immunostaining in Case 11 (40 post-conceptional weeks) with a chronic (glial scar) necrotic focus (*). Abnormal MBP immunostaining was in the form of globular segments (lines), rare tubules (arrowhead) and rare sheaths (arrows) (**D**). Note that the surrounding diffuse white matter (WM) is devoid of any MBP immunostaining (**B**–**D**). Image **A** is the Neurolucida image of this case; necrotic focus is highlighted. Image **B** is taken at 100×, scale = 200 μm; **C** is at 200×, scale = 100 μm; **D** is at 400×, scale = 50 μm.

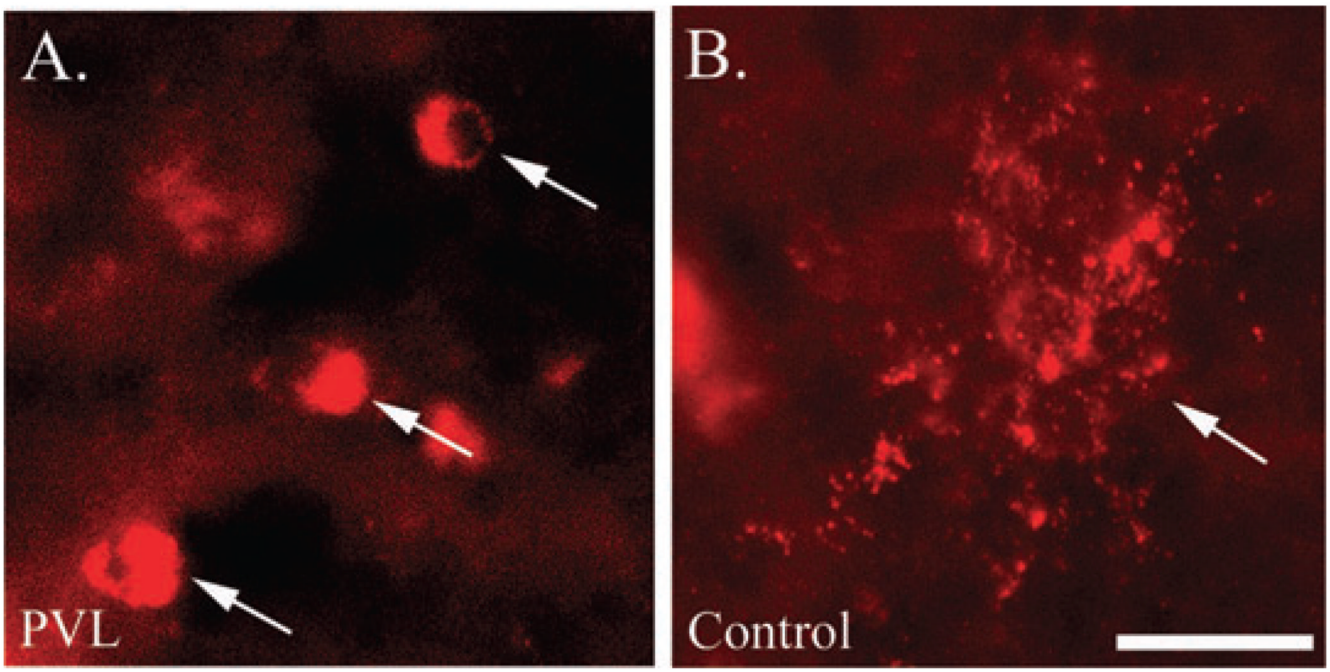

Figure 8.
O4 immunostaining of preOLs in a periventricular leukomalacia (PVL) (**A**) and control (**B**) case. The morphology of O4+ oligodendrocyte lineages (OLs) in the PVL case lack processes (arrows), whereas in the control case the processes are intact (arrow). Images are taken at 400×, scale = 25 μm.

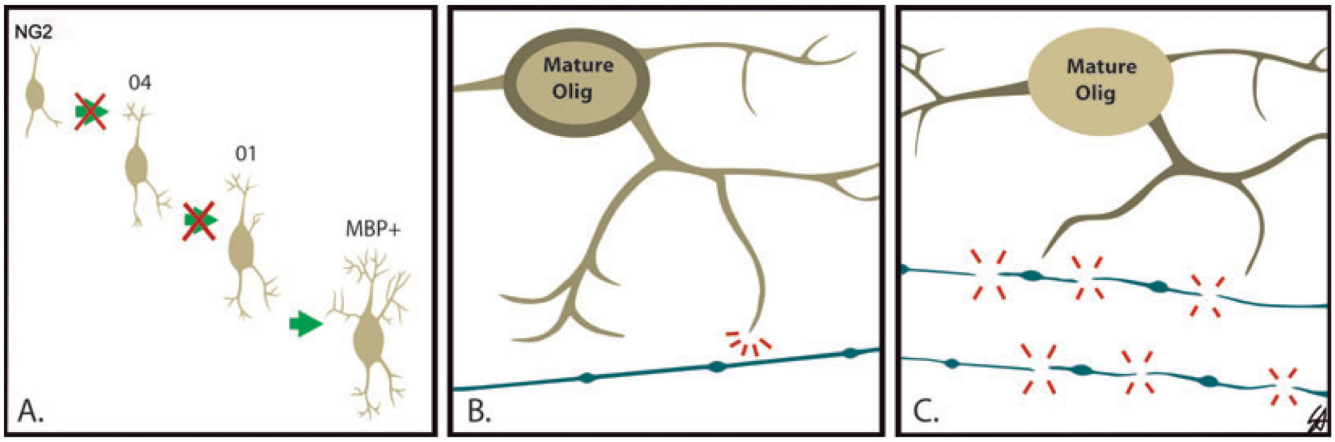

Figure 9.

Proposed hypotheses for the myelin deficits observed in long-term survivors of periventricular leukomalacia (PVL) in association with preserved Olig2 cell density. **A.** arrest in the maturation of the oligodendrocyte lineage (OL) progenitor (NG2) to a more mature myelin basic protein-(MBP) positive phenotype; **B.** inability of the mature OL to produce sufficient myelin [note hang-up of MBP (brown) in the perikaryon]; **C.** primary axonal injury leading to axonal-OL communication breakdown.

Table 1

Antibodies and lectin used in this study.

Antibody/lectin	Dilution	Source/catalog
Adenomatous polyposis coli (APC) (anti-mouse)	1:25	Calbiochem (OP80)
Caspase-3 (anti-rabbit)	1:20 000	BD PharMingen (551150)
CD68 (Kp-1) (anti-mouse)	1:50	Cell Marque (CMC 321)
Glial fibrillary associated protein (GFAP; anti-mouse)	1:10 000	Covance (SMI-22R)
GFAP (anti-rabbit)	1:200	DakoCytomation (Z0334)
Ki67 (anti-mouse)	prediluted	Zymed Laboratories (08–0156)
Ki67 (anti-mouse)	1:50	Novocastra Laboratories (NCL-Ki67-MM1)
Microtubule associated protein-2 (MAP-2); (anti-mouse)	1:200	Sigma (M-9942)
Myelin basic protein (MBP) (anti-mouse)	1:5 000	Covance (SMI-99)
Olig2 (anti-rabbit)	1:40 000	Dr C. Stiles, Boston, MA
O4 (anti-mouse)	1:1 000	Dr S. Pfeiffer, Farmington, CT
Tomato lectin (biotinylated)	1:200	Vector Laboratories (B-1175)
Vimentin (anti-mouse)	1:500	Chemicon (MAB 3400)

Table 2

Olig2 cell density (cells/mm^2) across the six boxes in periventricular leukomalacia (PVL) cases only.

Box	PVL (n = 18) (cells/mm^2)
1	138.7 ± 15.9
2	131.4 ± 15.6
3	128.5 ± 16.0
4	127.8 ± 17.0
5	123.5 ± 17.1
6	111.5 ± 17.0

The post-conceptional age-adjusted mean ± SEM of Olig2 cell density (cells/mm^2) decreased significantly across the six boxes in PVL cases ($P = 0.003$). Box 1 indicates the area overlying the necrotic focus, whereas Box 6 is the most distant (6 mm). $P < 0.05$ is considered significant.